# Temperature Effect on the Photocatalytic Degradation of Methyl Orange under UV-vis Light Irradiation

**HU Qi[1], LIU Baoshun[1, 2], ZHANG zhengzhong[1], SONG Mingxia[1], ZHAO Xiujian[1*]**

(1. Key Laboratory of Silicate Materials Science and Engineering, Ministry of Education, Wuhan 430070, China;

2. School of Materials Science and Engineering, Wuhan University of Technology, Wuhan 430070, China)

**Abstract:** PTA sol was prepared using titanium tetrachloride ($TiCl_4$), hydrogen peroxide ($H_2O_2$) and ammonia ($NH_3 \cdot H_2O$), and then stable anatase-$TiO_2$ hydrosol was synthesized by refluxing the PTA sol at 100 ℃. It was found that $TiO_2$ hydrosol can efficiently photo-degrade methyl orange (MO) under UV-vis light irradiation. Photocatalytic reactions at the temperature of 38 to 100 ℃ all followed pseudo-first-order rate law, and the temperature had a great effect on the reaction rate. The rate constants increased by about 6 times from $3.52 \times 10^{-4}$ to $2.17 \times 10^{-3}$ $min^{-1}$ when the temperature was adjusted from 38 to 100 ℃. Consequently, this photocatalytic course can be accelerated by using the infrared light of solar energy to increase the temperature of the photo-catalytic reaction, it should be a potential way to make full use of solar light in photocatalysis in practice.

**Key words:** photocatalysis; $TiO_2$; temperature; solar energy

## 1 Introduction

Nowadays, environmental issues have become one of the most important topics for the reason that pollutants from all over the world have been accumulating in living organisms and reaching harmful levels. Emphasis have been focused on technologies for the removal of the environmental pollutants such as adsorption, biodegradation, combined coagulation and flocculation, chlorination, ozonation, electrochemical oxidation, reverse osmosis, and also photocatalysis[1, 2]. In all these methods, photocatalysis is a promising one because it is an environmentally friendly process which can be driven by irradiation energy under ambient conditions.

$TiO_2$[3], as a photocatalyst, has attracted great attention from the world, and many researcher are devoting their efforts to developing this technology[4-7]. In comparison with other semiconductors, $TiO_2$ has been a dominant semiconductor photocatalyst due to its superior photocatalytic oxidation ability and nontoxic, non-photocorrosive and inexpensive characteristics[8-10].

There are many factors that can significantly influence the photocatalytic reaction[11-13], such as initial concentration, pH values, the grain size of photocatalysts, specific surface area, morphologies of photocatalysts and incident light intensity. Those factors have been studied deeply and extensively up to now. However, the effect of system temperature on photocatalysis has not attracted enough attention. In present research, it is found that the temperature has a great effect on the photodegradation of methyl orange. The photocatalytic efficiency can be increased about 5 times if the temperature increased from 30 ℃ to 100 ℃ Because the solar energy not only include UV light, which can be used to activate the photocatalytic course, but also contains the infrared light, which can be used to increase the temperature of photocatalytic system. In this way, we can make full use of solar energy in practice. This research is continuing in our group by enlarging its scale and using solar energy.

## 2 Experimental

### 2.1 Synthesis

The PTA sol was prepared using titanium tetrachloride ($TiCl_4$), hydrogen peroxide ($H_2O_2$, 30%) and ammonia ($NH_3 \cdot H_2O$, 3moL/L). Firstly, 6 mL $TiCl_4$ was added dropwise into ice-distilled water (400 mL, 0 ℃)

under magnetic stirring. The titanium hydroxide (Ti(OH)$_4$) was obtained by adding NH$_3$·H$_2$O into the titanium tetrachloride solution until its pH value was about 8. Secondly, the Ti(OH)$_4$ precipitate was filtered and rinsed by using distilled water for several times to remove the NH$_4^+$ and Cl$^-$ ions completely. Thirdly, the washed precipitate was dispersed well in distilled water (400 mL, room temperature). Afterwards, H$_2$O$_2$ was added slowly into the suspension. After continuous stirring for 24 h, the yellow and transparent PTA sol (Ti-H$_2$O$_2$ complex solution) was formed. Finally, the PTA sol was pyrolyzed and refluxed at 110 ℃ for 12 h until the milky TiO$_2$ hydrosol was gotten. The nano-TiO$_2$ powder dried at 40 ℃ from the TiO$_2$ hydrosol was used for characterizations.

## 2.2 Characterization

The crystal structure of the sample was identified by X-ray diffraction (XRD) with a diffractometer (type D/Max-RB) employing Cu-Ka radiation ($\lambda = 0.154056$ nm). The grain size $D$ were determined from the XRD pattern according to the Scherrer equation $D = K\lambda / \beta \cos\theta$, where $K$ was a constant (shape factor, about 0.9), $\lambda$ the X-ray wavelength (0.15418 nm), $\beta$ the full width at half maximum (FWHM) of the diffraction line, and $\theta$ the diffraction angle. $\beta$ and $\theta$ of anatase were taken from anatase (101) diffraction line, respectively.

The Brunauer-Emmett-Teller (BET) surface area ($S_{BET}$) and pore parameters of the TiO$_2$ powder were determined by nitrogen adsorption-desorption isotherm measurements at 77 K on a Micromeritics ASAP 2000 nitrogen adsorption apparatus. The sample measured was degassed at 180 ℃ before the actual measurements. Pore size distribution was calculated from adsorption branch of the isotherm by the Barrett-Joyner-Halenda (BJH) method using the Halsey equation.
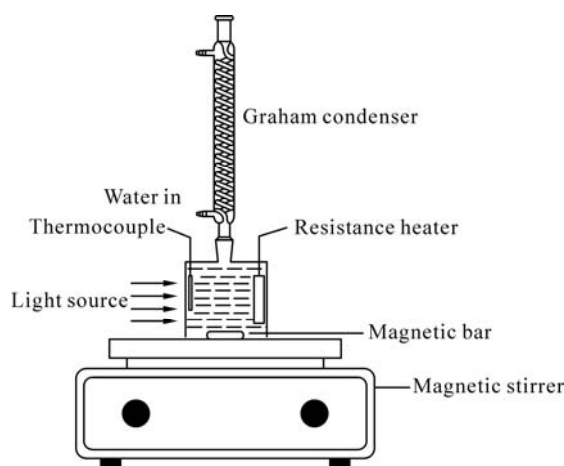


Fig.1 Photocatalytic reactor

## 2.3 Photocatalytic activity

Photocatalytic experiments with a 500 W Xe lamp (CHF-XM-500 W) as the light source were carried out by mixing 20 mL TiO$_2$ hydrosol to 80 mL MO aqueous solution (40 mg/L) , in a quartz glass reactor (Fig.1). The photocatalytic experiments were conducted accompanied by heating the mixture with a resistance heater and a thermocouple being used to heat the mixture and control the system temperature. A condenser was used to avoid the losing of the mixture due to evaporation. The distance between the light source and the reactor was 20 cm and the reactor was placed on a magnetic stirring machine. Prior to irradiation, the mixture was stirred by stirring in dark for 2 h to obtain the saturated absorption of MO. A series of certain volume of samples were withdrawn at certain time intervals for absorbance measurement by using a UV-vis spectrophotometer (Shimadzu UV-3101). The absorbance of the solution samples were used to determine the percentage of MO degradation. Moreover, the pseudo-first-order rate constant ($k$, min$^{-1}$) for the photodegradation reaction of MO was determined through the following relation[14]:

$$\ln\left(\frac{C_0}{C}\right) = kt \qquad (1)$$

where, $k$ can be calculated from the plot of $\ln(C_0/C)$ against time ($t$), $C_0$ and $C$ denote the initial concentration and reaction concentration, respectively.

# 3 Result and Discussion

## 3.1 Characterizations of TiO$_2$

The XRD pattern of the nano-TiO$_2$ powder is shown in Fig.2. The only detectable phase is anatase (JCPDS card no.21-1272) and the refractive peaks at 2$\theta$ of 25.4°, 38.0°, 48.0°, 55.0°, 62.8°, 70.2° and 75.8° are corresponding to (101), (004), (200), (211), (204), (220) and (301) lattice planes. The average grain size of TiO$_2$ particles that can be determined from the XRD pattern according to the Scherrer equation[15] is about 25 nm.
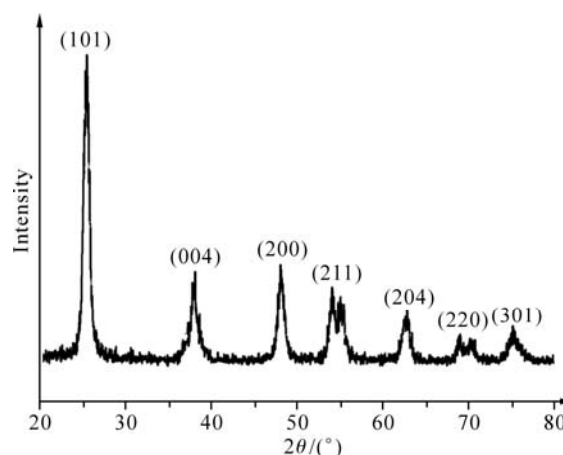


Fig.2 The XRD pattern of the nano-TiO$_2$ powder dried from TiO$_2$ hydrosol

Fig.3 shows the pore size distribution curve calculated from the desorption branch of a nitrogen isotherm by the BJH method using the Halsey equation[15]. The $S_{BET}$ of nano-TiO$_2$ powder is 199.8 m$^2$/g, which is much bigger than that of P25 (about 50 m$^2$/g).
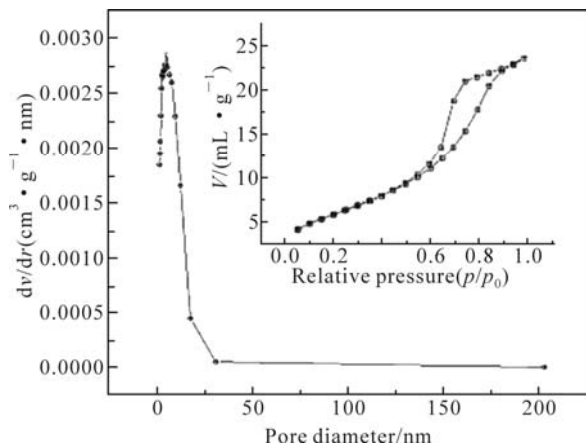


Fig.3 Pore size distribution curve and the corresponding isotherms (inset) of nano-TiO$_2$ powder dried from TiO$_2$ hydrosol

In summary, the XRD and BET analysis suggest that TiO$_2$ hydrosol synthesized contains well-crystallized and highly-dispersed anatase nano-TiO$_2$ particles with large $S_{BET}$, which is favorable for its superior photocatalytic oxidation ability.

### 3.2 Photocatalytic degradation of MO

The experiments showed that MO cannot be photodegraded if TiO$_2$ or UV light was not used, indicating that MO can not be pyrolyzed by heating with the heating temperature which was less than 100 ℃ and self-degraded by absorbing irradiation. Only when TiO$_2$ and UV light were both used, the MO can be efficiently degraded.
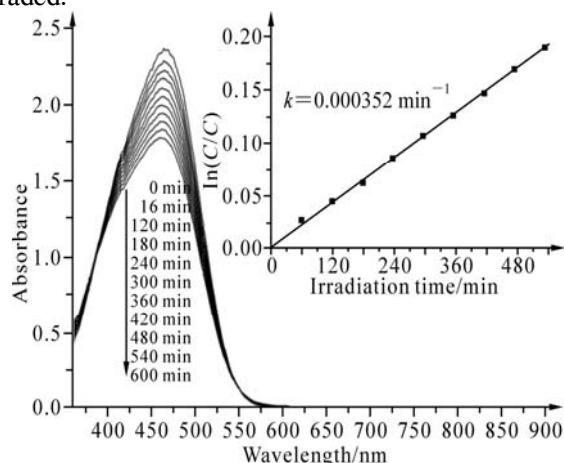


Fig.4 UV-vis absorption spectra of MO as a function of irradiation time at 38 ℃. Insert shows ln($C_0/C$) with respect to time

Fig.4 shows the change of UV-vis absorption spectra of remaining MO solution during the photocatalysis at 38 ℃, which were recorded after irradiation for a time interval of 60 min over a period of 540 min. The obvious decrease of absorbance peak centered at 550 nm shows that the TiO$_2$ hydrosol can serve as an effective photo-

catalyst. In addition, the linear feature of plots of ln($C_0/C$) versus time (Fig.5) indicates that this photocatalytic degradation reactions follow the pseudo-first-order rate law. The rate constant of the photocatalysis at 38 ℃ is $3.52 \times 10^{-4}$ min$^{-1}$.
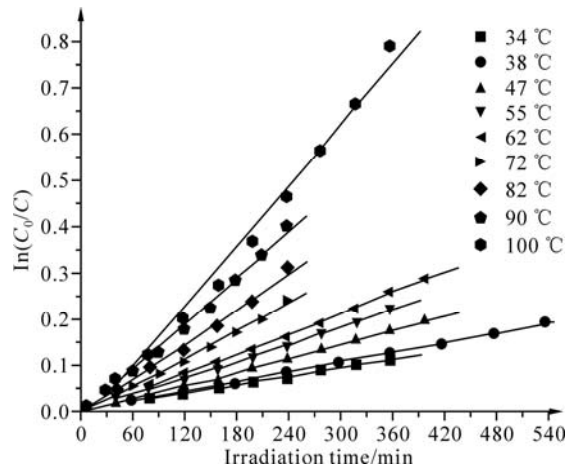


Fig.5 Plots of ln($C_0/C$) versus time at different temperatures

Further experiments were made to study the effect of temperature on the reaction rate of MO photodegradation and plots of ln($C_0/C$) versus time in the temperature range of 34 to 100 ℃ are showed in Fig.5. It can be seen that these data plots obtained at a certain experimental temperature can all be fitted into a line with a small error, which demonstrates that photocatalytic degradation of MO follows the pseudo-first-order law despite of the temperatures. The rate constant increases greatly from $3.12 \times 10^{-4}$ min$^{-1}$ to $2.17 \times 10^{-3}$ min$^{-1}$ over the temperature range of 34 ℃ to 100 ℃.

Fig.6 shows the Arrhenious-type plot from 307 K to 373 K. The arrhenious activation energy (Eact) deduced from the plot is about 27.69 kJ/moL, which is much bigger than that reported by Okamoto *et al* [16] for the photodegradation of phenol (10.0 kJ/mol) and by Al-Sayyed[11] *et al* for the degradation of 4-chlorophenol (5.4 kJ/moL). The high value suggests that thermally activation is important to accelerate the photodegradation of MO with TiO$_2$ as its catalyst and the adsorption/desorption processes are almost temperature- independent in this range.
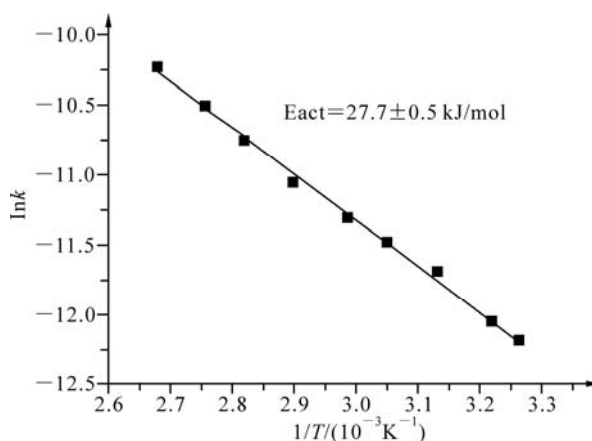


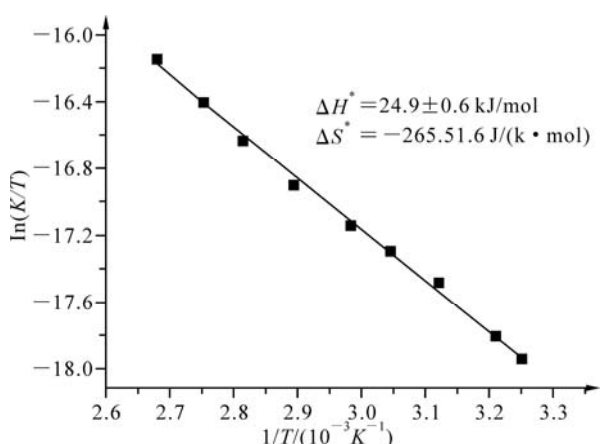Fig.6 Arrhenius (ln$k$ vs 1/$T$) plot for the photodegradation of MO

Fig.7 Eyring (ln(k/T) vs l/T) plot for the photodegradation of MO

Furthermore, the Eyring-type plot dependent on the temperature is shown in Fig.7. The data plots can be fitted into a straight line. Enthalpy and entropy of activation can be estimated according to eyring equation (2):

$$\ln\frac{k}{T}=-\frac{\Delta H}{R}\cdot\frac{1}{T}+\ln\frac{K_B}{h}+\frac{\Delta S}{R} \qquad (2)$$

where, $K_B$=Boltzmann's constant [$1.381\cdot10^{-23}$J/K], $T$=absolute temperature in degrees Kelvin ($K$), $h$=Plank constant [$6.626\times10^{-34}$ J·s], k the rate constant, $\Delta H$ and $\Delta S$ the enthalpy and entropy of activation respectively.

According to the above equation, a plot of ln(k/T) versus 1/T produces a straight line with the familiar form $y=-mx+b$ (Fig.7), where: $x=1/T$, $y=\ln(k/T)$, $m=-\Delta H/R$, $b=y$ ($x=0$).

So, $\Delta H$ can be calculated from the slop m of this line: $\Delta H=-mR$, And from the y-intercept:

$$y(x=0)=\ln\frac{K_B}{h}+\frac{\Delta S}{R} \qquad (3)$$

In this research, $\Delta H$=24.9 kJ/mol and $\Delta S$=−265.5 J/(k · mol), respectively. The large negative value of $\Delta S$ is consistent with a reaction between absorbed or photoabsorbed MO molecule and the surface oxidizing species photogenerated on $TiO_2$ particles during irradiation.

# 4 Conclusion

In summary, stable $TiO_2$ hydrosol synthesized by refluxing the PTA sol at a low temperature contains well-crystallized and highly-dispersed anatase nanoparticles. Increasing temperatue is greatly useful to the photocatalysis, and the rate constant can be promoted by about 6 times when the temperature was increased from 38 ℃ to 100 ℃. The arrhenious activation energy is as much as 27.69 kJ/mol, indicating the temperature can greatly affect the photocatalytic reaction of MO. In addition, Enthalpy and entropy of activation are 24.9 kJ/mol and −265.5 J/k·mol. Based on this research, the photocatalysis by both using the UV-vis and IR parts of solar energy is promising, which is now realized in our group.

# References

[1] L Hinda, P Eric, H Ammar, *et al*. Photocatalytic Degradation of Various Types of Dyes (Alizarin S, Crocein Orange G, Methyl Red, Congo Red, Methylene Blue) in Water by UV-irradiated Titania[J]. *Appl. Catal. B: Environ.*, 2002, 39(1): 75-90

[2] I K Konstantinou, T A Albanis. $TiO_2$-assisted Photocatalytic Degradation of Azo Dyes in Aqueous Solution: Kinetic and Mechanistic Investigations: A Review[J]. *Appl. Catal. B: Environ.*, 2004, 49(1): 1-14

[3] A Fujishima, K Honda. Electrochemical Photolysis of Water at a Semiconductor Electrode[J]. *Nature*, 1972, 238(5358): 37-38

[4] Jung-Yup Lee, Jaewon Park, Jun-Hyung Cho. Electronic Properties of N-and C-doped $TiO_2$[J]. *Appl. Phys. Lett.,* 2005, 87(13): 1-3

[5] T Umebayashi, T Yamaki, H Itoh, *et al*. Band Gap Narrowing of Titanium Dioxide by Sulfur Doping[J]. *Appl. Phys. Lett.*, 2002, 81(454):456–494

[6] R Asahi, T Morikawa, T Ohwaki, *et al*. Visible-Light Photocatalysis in Nitrogen-Doped Titanium Oxides[J]. *Science*, 2001, 293(5528): 269-271

[7] Ha Yong Lee, Yong Hwan Park, Kyung Hyun Ko. Correlation between Surface Morphology and Hydrophilic/Hydrophobic Conversion of MOCVD-$TiO_2$ Films[J]. *Langmuir*, 2000, 16(18): 7289-7293

[8] Junwang Tang, Zhigang Zou, Jinhua Y. Efficient Photocatalysis on $BaBiO_3$ Driven by Visible Light[J]. *J. Phys. Chem. C*, 2007, 111(34): 12779-12785

[9] T J Kuo, C N Lin, C L Kuo, *et al*. Growth of Ultralong ZnO Nanowires on Silicon Substrates by Vapor Transport and Their Use as Recyclable Photocatalysts[J]. *Chem. Mater.*, 2007, 19(21): 5143-5147

[10] F Gao, X Y Chen, K B Yin, *et al*. Visible-Light Photocatalytic Properties of Weak Magnetic $BiFeO_3$ Nanoparticles[J]. *Adv. Mater.*, 2007, 19(19): 2889-2892

[11] Ghassan Al-Sayyed, Jean-Christophe D'Oliveira, Pierre Pichat. Semiconductor-sensitized Photodegradation of 4-Chlorophenol in Water[J]. *J. Photochem. Photobiol. A: Chem.*, 1991, 58(1): 99-114

[12] J Saien, S Khezrianjoo, J Hazard. Degradation of the Gungicide Carbendazim in Aqueous Solutions with UV/$TiO_2$ Process: Optimization, Kinetics and Toxicity Studies[J]. *Journal of Hazardous Materials*, 2008, 157(2-3): 269-276

[13] H Seshadri, S Chitra, K Paramasivan, *et al*. Photocatalytic Degradation of Liquid Waste Containing EDTA[J]. *Desalination*, 2008, 232(1-3): 139-144

[14] Baoshun Liu, Liping Wen, Xiujian Zhao. The Study of Photocatalysis Under Ultraviolet + Visible Two-beam Light Irradiation Using Undoped Nano-titanium Dioxide[J]. *Mater. Chem. Phys.*, 2008, 112(1): 35-40

[15] Jimmy C Yu, Jiaguo Yu, Wingkei Ho, *et al*. Effects of F-Doping on the Photocatalytic Activity and Microstructures of Nanocrystalline $TiO_2$ Powers[J]. *Chem. Mater.*, 2002, 14(9): 3808-3816

[16] K Okamoto, Y Yamamoto, H Tanaka, M Tanaka and A Itaya. Heterogeneous Photocatalytic Decomposition of Phenol over $TiO_2$ Powder[J]. *Bull. Chem. Soc. Jpn.*, 1985, 58(7): 2015-2022

[17] Steffen Jockusch, Nicholas J Turro, Donald A Tomalia. Aggregation of Methylene Blue Adsorbed on Starburst Dendrimers[J]. *Macromolecules*, 1995, 28(22): 7416-7418